Measurements on drag reduction by use of a R2000 cone-plate rheometer

Maurits de Jong
s1795562
University of Groningen

July 23, 2012

Contents

1 Introduction

Every crew on a boat tries to minimize the traveling time between point A and B. So the crew have to improve the speed of the vessel by, for instance, saving in weight, more powerful engines or the reduction of drag. A disadvantage of reducing the weight as much as possible, is the decrease of the amount of safety, through less draft, the distance between the bottom of the hull and the water. Furthermore, weight can not always be decreased.

More powerful engines will increase the speed of the ship, but they consume a higher quantity of fuel, what increases the weight of the ship at the start of the journey and the total transport cost's for the owner. Furthermore, more powerful engines, or engines at all, are compatible or allowed at some ships.

Many research is done on drag reducing. Large vessels, like oil tankers or aircraft carriers, are specially designed with a bulbous bow at the front of the ship, so the bow waves will cancel out and as result there will be less drag from waves. Furthermore has every ship in the water to do with drag increasing effects caused by biofoiling, the growth of algae and other bio-organisms on the bottom of the hull of the boat, which increases the contact surface of the hull with the water. These bio-organisms cause a drag increase up to 60%, the speed will decrease up to 10% and the fuel consumption, if a engine is used, will increase up to 40%. The main solution to ensure that this effects will occur as little as possible is the use of anti-fouling. Anti-fouling is mostly a toxic coating which has the ability to kill the organisms which normally grow on the hull of the boat and prevent the drag-increase of the boat. A great disadvantage of these coatings is their toxic-level. They not only affect the organism on the hull of the boat, but they have a great impact on the rest of the biosphere of the salt an freshwater. Early very effective anti-fouling coating, like Tributyltin, were banned as coating because of its toxic-level and harmfulness on its environment. Also, a bio-fouling coating is a coating that will keep the organisms as long as possible away, so that the drag will not increase. These coatings give a great advantage for ships that are long in the water and are not often repaired or cleaned.

But these coatings only prevent or slow down the amount of drag magnifying effects, they not decrease the amount of drag. Nowadays, many research is done to find a save coating with the properties to decrease the drag. Almost every manufacturer of transport equipment, not only ships but also bicycle's, airplanes and cars. For example, Mercedes-Benz had made a car, based on the structure of the Ostraciidae. This box-like fish has a special body structure, which reduces the drag and allows him to swim more easily in the water. Big airplane manufacturers like Airbus, are engaged in research on riblets, small grooved lines, aligned in the directions of flow.

2 Theory

2.1 Boundary layers

The boundary layer is in fluid mechanics a layer of fluid around the surface of the object. For viscous environments, like water, the boundary layer is classified as the viscous boundary layer, denoted with the thickness δ. The thickness of the boundary layer is defined as the distance till the velocity of the flow is 99% of the freestream velocity. Even tough the boundary layer is very small compared the objects, most of the transport phenomena takes place here like heat transfer, mass transfer and the friction. A boundary layer can be laminar or turbulent. The fact if a boundary layer is laminar or turbulent are of major importance for the transport phenomena, and so for the friction in the solid/liquid interfaces. A laminar flow is mainly a ordered and predictable flow, which is easy to describe. For example a laminar flow occurs in a pipe, see figure 1.

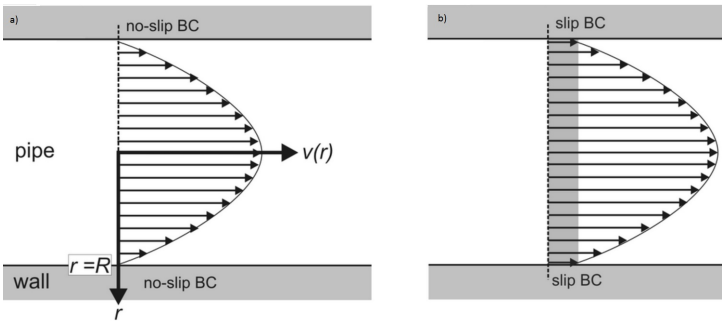

Figure 1: a) no-slip boundary condition in a pipe, b) slip boundary condition, with slip in a pipe.[1]

In the case of the no-slip boundary condition, when the adhesion between the solid and the fluid is greater than the cohesion of the fluid, the fluid at the boundary of the fluid-solid interface the same speed as the solid, so effectively no speed. The maximum speed with respect to the solid at its center.

A turbulent flow is more unsteady, chaotic and irregular and fast changing parameters like pressure and velocity, which makes it impossible to describe correctly. Due the chaotic nature of the flow, waves and vortices will work on the surface and increasing the shear stress. However, despite of the chaotic nature of a turbulent flow, at the surface of the solid there is a viscous sublayer with a more laminar nature. The state of the fluid, and hence the boundary layer, can be distinguished on its Reynolds number, Re. When the Reynolds number of the fluid is high, the flow will be turbulent. The Reynolds number can be discribed as:

$$Re = \frac{\rho \cdot v \cdot L}{\mu} \tag{2.1}$$

Here is ρ the density of the fluid, v is the speed of the flow, L is the hydraulic diameter and μ is the dynamic viscosity of the fluid. As $\mu = \nu \cdot \rho$, the equation will become

$$Re = \frac{v \cdot l}{\nu} \tag{2.2}$$

The Reynoldsnumber of the transition state from laminar to turbulent, Re_{tr}, depends on the geometry of the flow and among others, the structure of the surface and is specific for every experiment. To maintain as long as possible a laminar flow, researchers and developers try to maintain the highest transition Reynolds number. Phenning manufactured a pipe with $\mathrm{Re}_{tr} \cong 10^4$. Meseguer & Trefethen analyzed the problem up to $\mathrm{Re} = 10^7$[2]. Thus Re_{tr} depends, in pipes, only on the speed of the flow and the strength of the perturbations.

The amount a object in a flow suffers from drag can be described with a dimensionless constant, the drag coefficient, c_D. A higher c_D indicates that there is more drag. A typical value of c_D for ships is 0.80 0.85 for bulk carriers and 0.50 - 0.70 for a ferry boat. Newton suggested that with a known drag coefficient, it is possible to calculate the skin friction F_D, the amount of force necessary to transfer the momentum of the fluid to the solid, by the formula:

$$F_D = \frac{\rho \cdot v^2 \cdot C_D \cdot A}{2} \tag{2.3}$$

This formula only holds for flows with a laminar nature. The formula shows that the drag will increase fast, when the mean speed of the flow, or the boat, is increased by its square nature. To decrease the skin friction, mostly is tried to decrease the wetted surface, A, by removing the bio-fouling, or decrease the drag coefficient by use of special structures for surfaces or coatings.

2.2 Wenzel and Cassie-Baxter states

Water droplets occur in 2 states on a surface. When the droplets are full in contact with the surface, it is called the Wenzel state. Here is the droplet in contact with the entire surface, if the surface is flat or rough. When dealing with a rough surface, Wenzel proposed a a dimensionless factor, r, that represents the amount of roughness of a surface.

$$r = \frac{A}{A_{Geometric}} \tag{2.4}$$

Here is A the actual surface area and $A_{Geometric}$ the geometric surface area. Of course, for a perfect smooth surface with no bulges, $\mathrm{r} = 1$, but for every other case $\mathrm{r} > 1$. Due the increase of surface contact area, the angle of the water droplet will change, by the formula:

$$cos(\theta_{Wenzel}) = r \cdot cos(\theta) \tag{2.5}$$

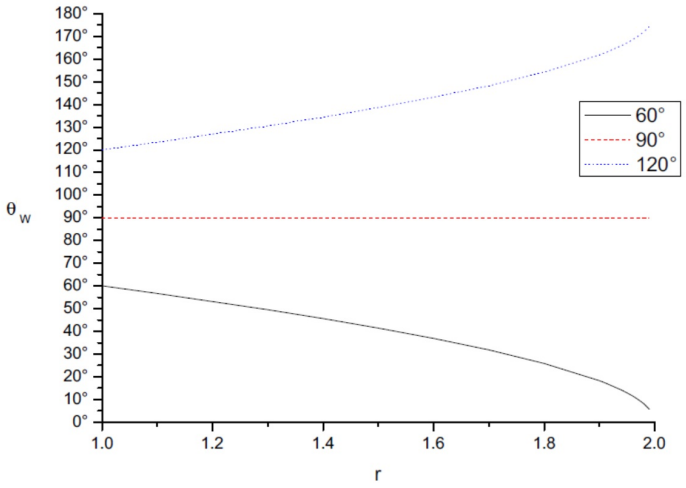

Figure 2: The contact angle θ_{Wenzel} as function of the roughness factor r, for $\theta = 60°, 90°$ and $120°$

This causes that the contact angle of a liquid on a smooth surface with $\theta < 90°$ will decrease when the surface become rougher and the contact angle will increase when $\theta > 90°$, see figure 2

When the droplet only touches the tops of the peaks of the rough surface, it is called the Cassie-Baxter state.[3] Under the droplets in the Cassie state, there are air cavities trapped between the peaks of the rough surface, which enlarge the hydrophobic effect. See figure 3. When in the Cassie & Baxter state, the droplet is partly in contact with the solid and partly with the air. When r' is the fraction of the droplet that is in contact with the solid and η is the fraction of the droplet that is in contact with the air, the contact angle of a droplet in the Cassie & Baxter state can be calculated:

$$cos(\theta_{CB}) = r' \cdot cos(\theta) + \eta \cdot cos(\theta_{air}) \tag{2.6}$$

r' and η together is of course equal to 1. Since a water droplet in full contact with air has a contact angle of 180°, the formula can be simplified to:

$$cos(\theta_{CB}) = r' \cdot cos(\theta) - \eta \tag{2.7}$$

Whether a droplet occur in a Wenzel of Cassie & Baxter state depends on a few factors. When a surface become to rough, it is energetically more sufficient for the water droplet to be in the Wenzel state than the Cassie & Baxter state. It is suggested that there is a critical contact angle, θ_c, for the transition, defined by:

$$\theta_c = \frac{r' - 1}{r - r'} \tag{2.8}$$

However often a droplet occur not in the energetically most ideal state. Since this state is very instable, the droplet changes irreversible to the energetically more ideal state when applying pressure on the droplet.

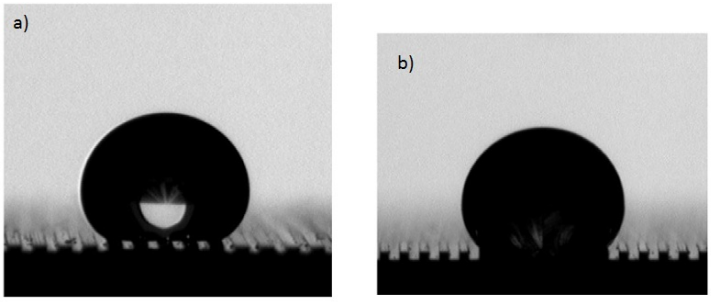

Figure 3: a) droplet on a rough surface in Cassie state, b) droplet on a rough surface in Wenzel state.[4]

When a droplet is on a surface, it has the contact surface A, whether it is in a Wenzel or Cassie & Baxter state. When the contact surface will be enlarged with dA, a certain amount of work had to be done, calculated by:

$$\delta W = \gamma \cdot dA \tag{2.9}$$

Here is γ the surface tension. As a result, droplets with a small contact area and surface tension, will flow of easy from the surface. Another advantage is the increase in difficulty for dirt or filth to attach to a wall, or for bio-organism to the hull of a boat. For example, the recently launched superhydrophobic coating Neverwet^{TM} of Ross Nanotechnology has the promising effect that water, or mud, is unable to attach itself on the coated objects.

2.3 Structured surfaces

To investigate drag reduction by the structure of the surface, many research is done on the surface of the objects and have led to fabrication of superhydrophobic surfaces with unusual properties of the contact angle of the droplet with the surface. When the contact angle $\theta > 90°$, the surface is hydrophobic. The contact angle is the angle the droplet makes with the surfaces. When $\theta > 150°$, the surface will become superhydrophobic, the droplet tries to make as less contact with the surface through becoming a sphere. The contact angle the droplet makes with a smooth surface can be calculated by the Young's equation:

$$\cos(\theta) = \frac{\gamma_{SG} - \gamma_{LS}}{\gamma_{LG}} \tag{2.10}$$

Here are γ_{SG}, γ_{LS} and γ_{LG} the interfacial tensions of the solid-gas, liquid-gas and the solid-liquid interface. When there is only a gas-liquid interface, the

droplet become a circle with $\theta = 180°$. For droplets on solids the case of $\theta = 180°$ occurs when $\gamma_{LG} - \gamma_{SG} = \gamma_{LG} > 0$. Researchers at the university of Massachusetts were able to manufacture a solution of nano particles $MeSiCl_3$, which caused, after applied to a surface, a completely hydrophobic environment with the same contact angle as if the droplet was surrounded by air, so $\theta = 180°$.[5] Unfortunately, this coating is not available for commercial use. Normal teflon, used for cooking ware and anti-fouling, has a contact angle of approximately $\theta = 110°$.

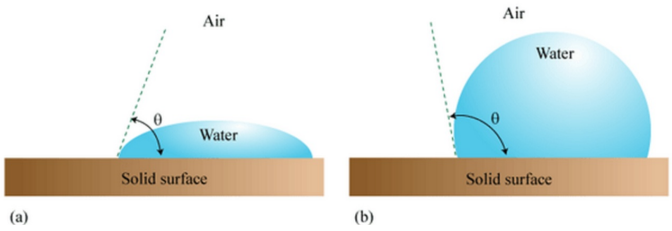

Figure 4: Image of a) a droplet on a hydrophilic surface, b) droplet on a hydrophobic surface

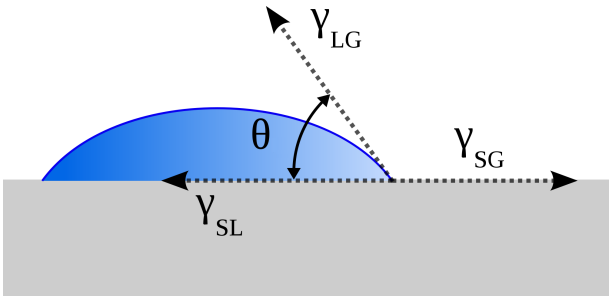

Figure 5: The interfacial surface tensions of a droplet

Superhydrophobic surfaces repel water droplets in such a extent, that in approximation the no-slip boundary condition can be achieved.

This research, inspired by the selfcleaning effect of the lotus leave and the skin of sharks, which allows the shark to swim in water with a small amount of drag in comparison with other fishes with a smoother skin, and are able to achieve a higher speed with the same amount of energy. By investigating the sharkskin and the lotus leave, researchers noticed that both have a structured surface, what was against the theories of skin friction of that time, because smoother surfaces tend to cause smaller skin friction F_D, due the smaller wetted area A, see equation 2.3. However. The theory then suggested that to achieve a surface which the least amount of skin friction at the solid-fluid boundary, the

surface has to be as smooth as possible, as bulges and obstacles would increase the amount of drag. This is true for large bulges, but when the size of the bulges become below a certain level, depended on the fluid and the speed of the fluid, the surface become more or less superhydrophobic and the drag coefficient will decrease. The decrease of C_D compensate the increase of the wetted area. These results are among others achieved with simple sandpaper [7] and riblets.

One of the most common ways of making a hydrophobic surface is by use of lithography. Figure 6 shows a SEM-picture of rough surface, made of a pillar like structure. Another method to produce a hydrophobic structure is by making a mixture of hydrophobic colloids and some sacrificial colloids. B. P. van der Wall[13] describes a method by use of 200 nm Teflon® colloids and a wide range of different sized polysterene sacrificial colloids, varying from 0.1 nm till 25.7 nm. The sacrificial colloids in the applied mixture were removed by heat degeneration by use of a hotplate. The contact angle increased by use of this method from 115° (normal Teflon layer) to 125° (Teflon layer with colloids) to eventually 170°, (heated Teflon colloids and sacrificial colloids mixture). A third way to manufacture hydrophobic coatings, is to use a contained spin-coater. A cooled disk with the coating is placed with a beaker with a boiling liquid. When spinning the disk, the liquid droplets condensate on the disk, leaving holes behind after the procedure. Although increasing the contact angle up to 30°, this method cause not the same increasing properties as other methods.

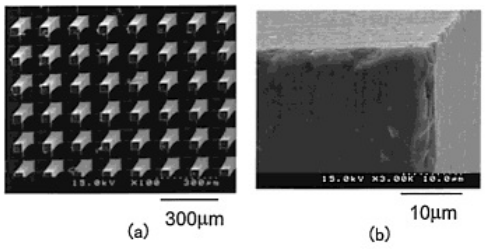

Figure 6: SEM image of a pillar like surface: a) low-magnification image, b) high-magnification image.[6]

2.4 Riblets

At the time of the oil crisis in the 1970s, NASA was begun to investigate the structure of the sharkskin to find a way to reduce the drag on aircrafts and wings. They were able to manufucture the first so called riblets. Riblets are small, long, lines, aligned to the direction on the flow of the fluid. Researchers measured a reduction in the skin friction by use of these riblets. There are a few different kind of structures made of riblets, where measurable drag reduction is noticed. The most common are the triangular, the semicircular, the trapezoid and the blade riblets, each of them have their own optimum range as parameters. The optimum non dimensional riblet width, s^+, is of great importance to calculate

the optimal spacing and width of the riblets. Researchers had discovered that every type of riblet has its own optimum value of s^+, see figure 8. For all the types of riblets, the optimum value varies between the 15 and 20.

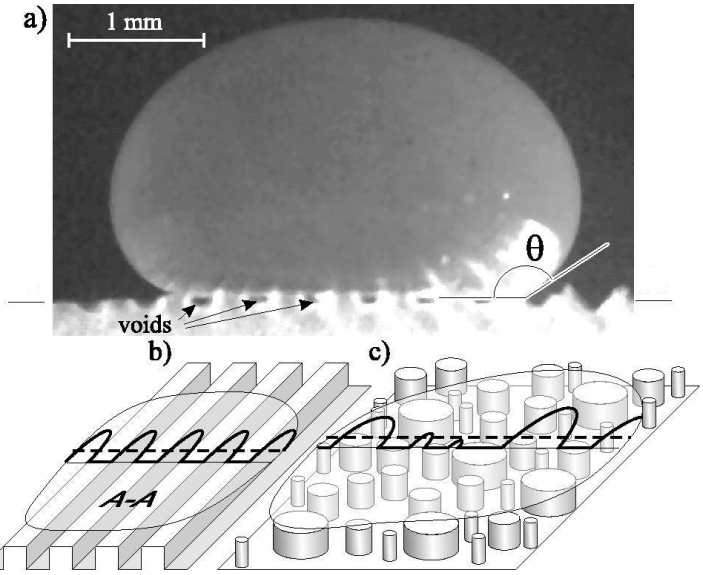

Figure 7: Droplet on a rough surface: a) a droplet on a rough surface, where θ is the contact angle of the droplet with respect to the boundary, b) perspective view of riblets showing the fluid velocity profile, where the dashed line is the average slip, c) perspective view of a irregular surface showing the fluid velocity profile.[8]

The absolute width is depended on non dimensional riblet width by:

$$s = \frac{s^+ \cdot \nu}{u_{\tau 0}} = \frac{s^+ \cdot \nu}{\sqrt{\frac{\tau_0}{\rho}}} \tag{2.11}$$

Where ν is the dynamic viscosity, $u_{\tau 0}$ is the near wall shear stress, ρ the density of the fluid and τ_0 wall shear stress at a smooth surface. A commercial airplane, where air causes most of the drag, has a optimum as spacing of approximately 90 μm.[9] Ships and boats however, due the far more denser water, have a lower spacing, depending on the density of the liquid and the speed of the boat, between the 5 μm and 20 μm. Furthermore, the dimensionless height parameter, h^+, is necessary to calculate the optimum peak height values. With this the optimum $\frac{h}{s}$ ratio can be calculated. For the triangular riblets this value is approximately 1, depending on the angle of the riblets, for semicircular it varies between 0.5 and 0.7, depending on the kind of the circular is used, for trapezoid around 0.5, more if the angle of the riblets is lower, and for the blade like riblets the optimum $\frac{h}{s}$ ratio is 0.5. As can see in figure 8, most drag reduction can be achieved by use of blade like riblets. Unfortunately, due its

h

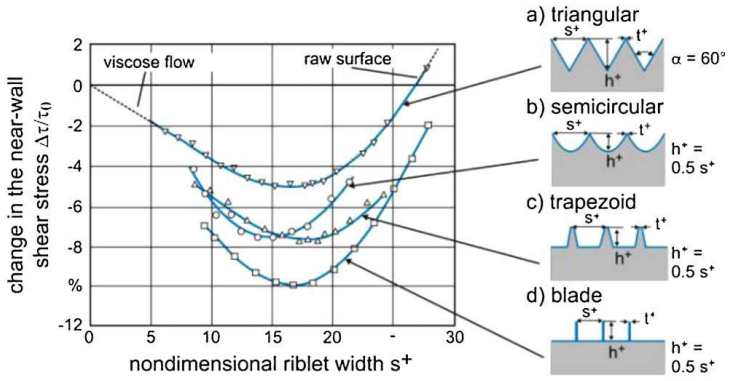

Figure 8: Change in shear stresses for different riblet structures.[9]

fragile structure, it will easy crack and makes it less suitable for commercial applications.

When investigating the nature of riblets, researchers noted that riblets do not always decrease the drag. Every riblet type has its own optimum $\frac{h}{s}$ ratio, among others depending on the speed of the flow. If the speed decrease and the flow become more laminar instead of turbulent, the riblets lose their ability to decrease the amount of drag and begin to increase the drag. This is also the case if the wrong parameters are used for riblets. In 1999 Lee *et all* were investigating the location of vortices in flow with respect to the riblets of two with semi-circular riblets coated surfaces.[10] Here was one plate coated with a drag decreasing structure ($s^+ = 25.2$ in this case) and one with a drag increasing structure ($s^+ = 40.6$). For the case of the drag decreasing riblets, Lee noted that the vortices in flow occured mostlu above the riblet structure due the Cassie & Baxter state of the riblets. Most of the shear stress of the vortices is applied on the fragile top of the riblets peaks. Lee suggested that the drag decrease will be larger when the riblets are made thinner, but by this more fragile and more likely to crack. The case for the drag increasing riblets, when the riblets caused a Wenzel state, the vortices occured between the riblets, what increased the wetted area and the shear stress.

3 Experiments

3.1 Rheometer

To measure the drag reduction of surfaces, coated with riblets, many researchers use a rheometer to measure the drag reduction.[11] A rheometer is normally used

by chemist to measure the shear stress and the viscosity of a sample, but since the viscosity was already known (ν of water is 1.004 $\frac{m^2}{s}$) en kept constant by keeping the temperature constant (T = 20° C) by using a peltierplate, it was possible to measure the differences of the skin friction between the samples. See figure 9.

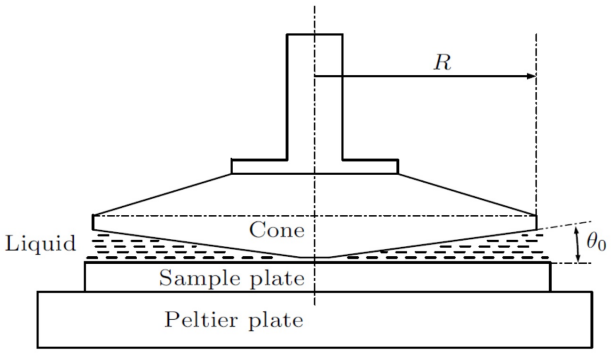

Figure 9: Schemetic draw of a rheometer.[11]

The samples were placed in the apparatus, beneath a constant spinning cone with an angle of 2° and a radius of 2.0 cm. The cone with the lowest angle and the highest radius available was used, since the viscosity of the liquid we used, demineralised water, is very low compared the liquids normally used in rheometers. The apparatus that was used was a R2000 cone-plate rheometer of TA industries.

For the experiment a few samples were made with different surface structures or coatings. Disk 1 had a surface structure based on the riblets, where the riblets where composed on the disks in concentric circles. See figure 10. Disk 1 has a $\frac{h}{s}$ ratio of $\frac{1}{15}$, what is far off the optimum $\frac{h}{s}$ ratio of. Disk 2 has a $\frac{1}{2}$ ratio, the optimum ratio and was designed with the appropriate sizes for the spacing and the height of the riblets. Furthermore, disk 3, a disk with no surface structure is produced as reference disk and there were measurements done on a disk, coated with the coating used on the skûtsje named *VC Offshore with Teflon*, disk 4.

Disk	Average Height	Average Spacing	$\frac{h}{s}$ ratio
1	2 μm	30 μm	$\frac{1}{15}$
2	12.5 μm	25 μm	$\frac{1}{2}$
3	0	-	-
4	0	-	-

Table 1: Structure of the disks

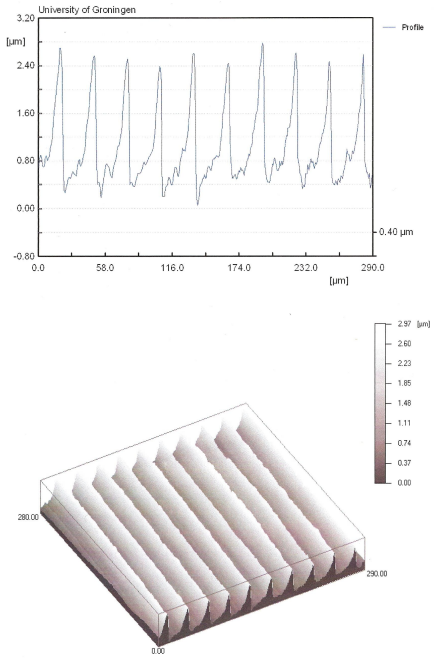

Figure 10: Disk 1: h = 2 μm and s = 30 μm

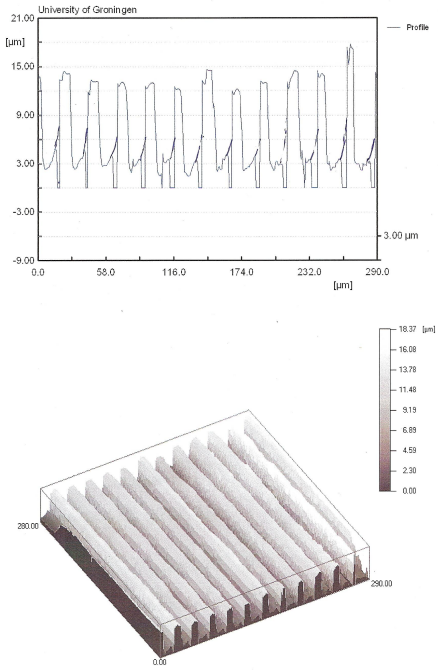

Figure 11: Disk 1: h = 12.5 μm and s = 25 μm

3.2 Results

To ensure that we work in the regime of the rheometer, we first measured the dynamic viscosity, η, of all the disks. Figure 12 shows the average dynamic viscosity of all the disks as function of different shear stresses. Disk 3, the disk with no coating or coated surface, has to be closed to the value of dynamic viscosity of water of 20° C, η = 1.002 * 10^{-3} Pa s. However, due the fact a liquid with a very low viscosity is used, the apparatus works in its error regime, what causes that the measurements done with the higher shear rate are more accurate. Table 2 shows the average values of the different disks.

Disks	Average dynamic viscosity
Disk 1	1,21*10^{-3} Pa s
Disk 2	9,31*10^{-4} Pa s
Disk 3	1,39*10^{-3} Pa s
Disk 4	8,17*10^{-3} Pa s

Table 2: Structure of the disks

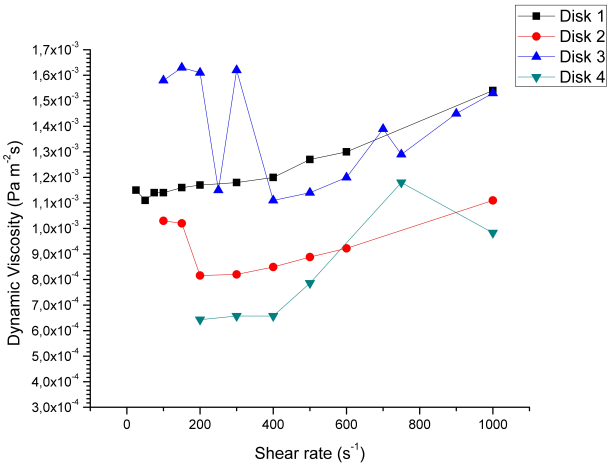

Figure 12: Graph of the dynamic viscosity of the 4 disks as function of their shear rate.

To measure the drag of the different disks, the torque has to be measured. It was possible to measure the shear stress as function of the shear rate, $\dot{\gamma}$, is which is inversely dependent on the angular velocity by $\dot{\gamma} = \frac{\omega}{\theta}$. Figure 13 shows the shear stress of disk 4 at a shear stress of 1000 s^{-1} over a time of 10 minutes.

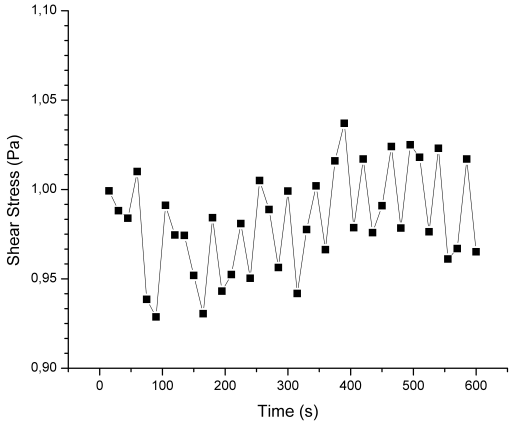

Figure 13: Graph of the shear stress of disk 4 at a shear rate of 1000 s^{-1} as function of the time.

For a rheometer, which uses a spinning cone and a plate to calculate the shear stress, the torque, M, of the disks are dependent on the shear stress, τ, and the radius, r, of the cone of the rheometer by:

$$M = \tau \frac{2}{3} \pi r^3 \tag{3.1}$$

Figure 14 shows the values of the torque found for the different disks as function of the shear stress.

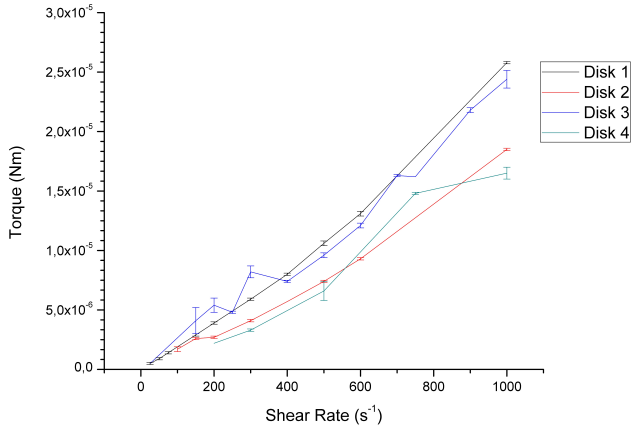

Figure 14: Graph of the torque of the 4 disks as function of their shear rate.

Not only the torque itself is important to find the drag reduction. The relative drag reduction compared to the reference disk can be calculated by:

$$\kappa_{torque} = \frac{M_{reference} - M_{disks}}{M_{reference}} * 100\% \tag{3.2}$$

κ_{torque} stands here for the torque reduction, $M_{reference}$ for the torque of the reference disk, disk 3, and M_{disks} for disk 1, disk 2 and disk 4. Figure 15 shows the percentage torque reduction compared to the reference disk as function of its shear rate.

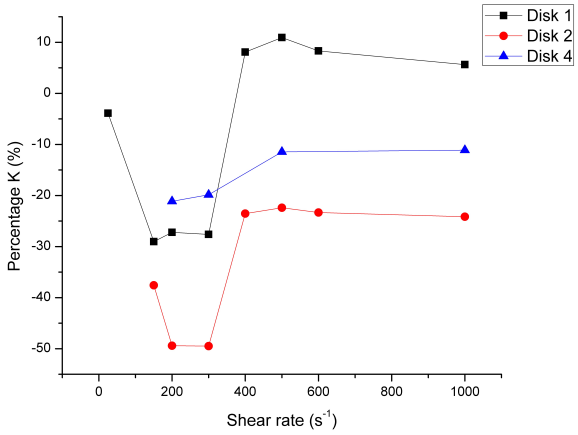

Figure 15: Graph of the percentage torque reduction of the disks.

3.3 Discussion

Figure 14 shows that disk 2, the disk with the riblets with the proper $\frac{h}{s}$ ratio, experience the least torque as expected when comparing with disk 1, the disk with not the proper $\frac{h}{s}$ ratio. When comparing the disk with the coating with the reference disk, that disk experience less torque. Disk 4, coated with *VC Offshore with Teflon*, shows also a drag reduction ranging from 13% up to 22% compared to disk 3. That the disks experience less drag meet the expectations, as they all have a higher contact angle. However, the disks experience far less drag than expected. The graph shows that disk 2 has the unlikely drag reduction of approximately 50 percent% at his maximum and 25%. As expected disk 2, the disk with the appropriate $\frac{h}{s}$ ratio shows more reduction in the torque than disk 1. However researchers had manufactured riblet structures, which caused a maximum drag reduction of about 18%[8], what is far below the 50%. Surfaces which increase the drag reduction work in the turbulent regime of flows, so it is also necessary to calculate if the flow in the rheometer is really turbulent. B. Frohnapfel described a way to calculate if the flow in a cone-plate rheometer is really turbulent by: $\tilde{\mathrm{R}} = \frac{\dot{\gamma} \cdot \rho \cdot r^2 \cdot \theta^3}{12\mu}$.[12] Here is $\tilde{\mathrm{R}}$ a dimensionless number, which has to be $\tilde{\mathrm{R}} > 4$ for a fully turbulent environment, r the radius of the cone, θ is the angle of the cone, $\dot{\gamma}$ the shear stress and μ the dynamic viscosity and ρ the density. $\tilde{\mathrm{R}}$ for the case with the highest shear rate, 1000 s^{-1}, the case when the flow is the most turbulent, equals to 1.418. Taking in account the average measured value of the dynamic viscosity of disk 3 with a shear rate of 1000 s^{-1}, $\mu = 1,53 * 10^{-3}$, $\tilde{\mathrm{R}} = 0.927$. Both values are beneath the minimum value of $\tilde{\mathrm{R}}$, so the flow was not turbulent at all. Between the values $\tilde{\mathrm{R}} = 1$ and $\tilde{\mathrm{R}} = 4$, there is a transition state where the flow is partly turbulent and partly laminar. Unfortunately, when measured value of μ is used, $\tilde{\mathrm{R}}$ did not even fall in the transition state. Since drag reducing effects only occur in the turbulent regimes, the rheometer must measured very little till no drag reduction. Since the rheometer was doing measurements in its error regime, it is far more likely that the rheometer did not do any correct measurements at all. This can be avoided, when a rheometer is used with a smaller cone-angle and a greater cone-diameter.

4 Conclusion

Nowadays, many research is done on the use of drag reducing coatings for airplanes, cars and ships. The promising riblet structure cause a drag reduction up to 18%. Unfortunately, despite of the great advantages of this products, riblets are not on great scale commercial producible and they are hard to attach to surfaces. More promising are the coatings based on a mixture with nano particles, which could cause a complete hydrophobic environment for solids. Unfortunately, the coatings with the most promising effects are not available yet. Fortunately, these subjects have caused a lot of interest by large companies, who are spending a lot of research to make this coatings more available,

cheaper and usable. It is noted that coatings which make use of colloids in the coating have a hydrophobicity increasing effect. The coating that is used at this time, *VC Offshore with Teflon* has some hydrophobic properties, however they can be increased by use of nano particles or new coatings like the recently launched coating Neverwet or other water repellent coatings as *Lotus-Effect*®, that is based on the leaves of the lotus flower.

References

[1] S. Berg *et al*, *Flow in porous media with slip boundary condition*, Shell International Exploration and Production B.V., the Netherlands.

[2] Trinh *et al*, *On the critical reynolds number for transition from laminar to turbulent flow*, Massey University, New Zealand.

[3] Takahiro Koishi *et al*, *Coexistence and transition between Cassie and Wenzel state on pillard hydrophobic surface*, University of Fukui, Fukui, 2009

[4] Ashiqur Rahman *et al*, *Drainage of frost melt water from vertical brass surfaces with parallel microgrooves*, University of Illinois, Urbana-Champaign, 2011

[5] Lichao Gao and Thomas J. McCarthy, *A perfectly hydrophobic surface* ($\theta_A/\theta_R = 180°/180°$, University of Massachusetts, Amherst, Massachusetts, 2006.

[6] Zen Yoshimitsu *et al*, *Effects of Surface Structure on the Hydrophobivity and Sliding Behavior of Water Droplets*, University of Tokyo, Tokyo, 2002.

[7] Robert J. Daniello, *Drag reduction in turbulent flows over micropatterned superhydrophobic surfaces*, University of Massachusetts, Amherst, 2009.

[8] Salil Gogte *et al*, *Effective slip on textured superhydrophobic surfaces*, The university of New Mexico, Albuquerque, New Mexico, 2005.

[9] Berend Denkena, *et al*, *Manufacturing of functional riblet structures by profile grinding*, Leibniz Universität Hannover, Hannover, 2010

[10] S.-J. Lee & S.-H. Lee, *Flow field analysis of a turbulent boundary layer of a riblet surface*, Pohang University of Science and Technology, South Korea, 1999.

[11] Xue Wen Hui, *et al*, *Mechanism Analysis of One-Dimensional Quasiperiodic Groove Drag-Reduction*, Northwestern Polytechnical University, Xi'an, 2010

[12] B. Frohnapfel *et al*, *Experimental investigations of turbulent drag reduction by surface-embedded grooves*, Cambridge University, Cambridge, 2007.

Books used:

[13] B. P. van der Wal *Static and Dynamic Wetting of Porous Teflon®*, 2006, ISBN: 90-367-2861-4.

[14] Pierre-Gilles de Gennes, Françoise Brochard-Wyart and David Queéré, *Capillarity and Wetting Phenomena, Drops, Bubbles, Pearls, Waves*, 2002, ISBN: 0-387-00592-7.

[15] G. Hauke, *An Introduction to Fluid Mechanics and Transport phenomena*, 2008, ISBN: 978-1-4020-8536-9.